GEOLOGICA CARPATHICA, JUNE 2019, 70, 3, 261–276 doi: 10.2478/geoca-2019-0015

The Upper Cretaceous intrusive rocks with extensive crustal contribution in Hacımahmutuşağı Area (Aksaray/Turkey)

SERHAT KÖKSAL

Middle East Technical University, Central Laboratory, R&D Research and Training Center, Radiogenic Isotope Laboratory, TR-06800, Ankara, Turkey; skoksal@metu.edu.tr

(Manuscript received January 9, 2019; accepted in revised form April 23, 2019)

Abstract: The Hacımahmutuşağı area (Aksaray/Turkey) is located in the western part of the Central Anatolian Crystalline Complex (CACC). Gneiss and marble compose the basement units, while intrusive rocks are gabbros and granitoids. The pegmatitic hornblende gabbros contain pegmatitic to fine-grained hornblendes, plagioclase, clinopyroxene, and accessory opaque minerals. The fine-grained gabbros, on the other hand, are composed of plagioclase, hornblende, and biotite as major components whereas the apatite and opaque minerals are present in accessory content. Granitic–granodioritic rocks are the common intrusive rock types in the area, and constitute quartz, orthoclase, plagioclase and biotite, and accessory zircon and opaque minerals. Leucogranites, comprising quartz, orthoclase, plagioclase with minor biotite, hornblende, and with accessory apatite and opaque minerals, are found as dykes intruding the marble and the granitic–granodioritic rocks. Strontium–neodymium isotope data of gabbros and granitoids have high $^{87}Sr/^{86}Sr_{(i)}$ ratios (0.7076 to 0.7117) and low $\varepsilon Nd_{(i)}$ values (−5.0 to −9.8) point out enriched source and pronounced crustal contribution in their genesis. In the Hacımahmutuşağı area, it is plausible that the heat increase caused by the hot zone, which was generated by underplating mafic magma along with the hydrous mafic sills in the lower crust, might have resulted in partial melts from crystallized mafic sills and older crustal rocks. It can be suggested that these hybrid melts adiabatically rose to the shallow crust, ponded and crystallized there and formed the magma source of the intrusive rocks within the Hacımahmutuşağı area and the other hybrid granitic rocks with crustal signatures in the CACC. Geochemical data indicate that granitoids and gabbros are collision to post-collision related sub-alkaline rocks derived from an enriched source with extensive crustal inputs.

Key words: Hacımahmutuşağı, Central Anatolia, granitoids, gabbros, Sr–Nd isotopes.

Introduction

Intrusive igneous rocks are common rock types in the earth's crust and exist in various tectonic settings, ranging from subduction and collision related regions to intra-continental areas (e.g., Pitcher 1979; Pearce et al. 1984). They have particular importance in complex tectonic regimes like Alpine Orogenesis, which was effective in Central Anatolia (Turkey) during the closure of the Neotethyan Ocean in the Late Cretaceous (e.g., Moix et al. 2008; Göncüoğlu et al. 1997a, 2015). Traces of this belt were recorded within the ophiolitic units overthrusting the basement units and the related igneous rocks in the Central Anatolian Crystalline Complex (CACC) (e.g., Göncüoğlu et al. 1997a, 2010; Yalınız et al. 2000; Robertson et al. 2009). In Central Anatolia, igneous rocks outcrop in various places and their relationships with the other units preserve evidence of the geodynamic evolution of the region in spite of the extensive Eocene and post-Eocene tectonic/magmatic activities (e.g., Boztuğ et al. 2009). Their petrological characteristics are not only important in linking to regional geodynamics but also in understanding the petrogenesis and formation processes of similar igneous rocks in the world.

Hacımahmutuşağı is a small town in West-Central Anatolia, but it is one of the key areas for description of the common igneous rocks and their petrogenetic characteristics in the CACC (Fig. 1). Previous studies in the Hacımahmutuşağı area focused on geological and petrographical studies with limited geochemical and geochronological data (e.g., Köksal 1992; Köksal et al. 2001; Kadıoğlu et al. 2003). The aim of this study is to investigate the petrology of the intrusive rocks in the Hacımahmutuşağı area with new geochemical, including isotopic, data and to provide new insights into the geodynamic approaches for the CACC.

Regional geology

Turkey covers a geologically noteworthy region since it is in the junction between Eurasia and Gondwana (e.g., Göncüoğlu et al. 1997a; Okay & Tüysüz 1999; Bozkurt & Mittwede 2001). Alpine orogenesis related to the closure of the various branches of Neotethys shaped the geology of the region especially during the Late Cretaceous (e.g., Moix et al. 2008; Göncüoğlu et al. 2015). Pontides in the northern part of the country represent the active south margin of Eurasia, which is bounded by

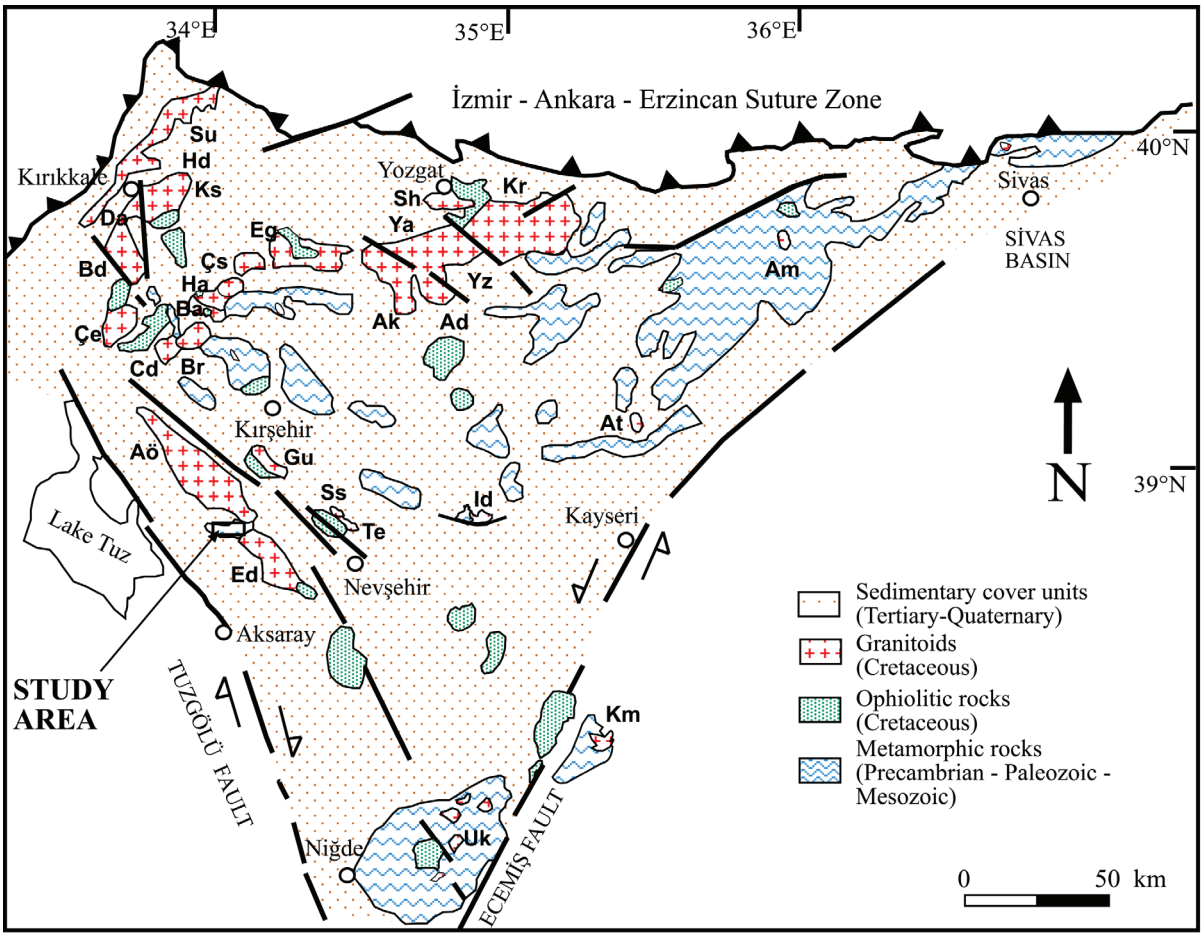

Fig. 1. Geological map of the CACC (after Bingöl 1989; Göncüoğlu & Türeli 1994). Central Anatolian granitoids: Ad — Adatepe; Ak — Akçakoyunlu; Am — Akdağmadeni; Aö — Ağaçören magmatic association; At — Atdere; Bd — Behrekdağ batholite; Br — Baranadağ; CD — Cefalıkdağ; Çe — Çelebi; Çs — Çamsarı; Da — Danacıobası; Eg — Eğrialan; Ed — Ekecikdağ magmatic association; Gu — Gümüşkent; Ha — Hamit; Hd — Hasandede; Id — İdişdağ; KM — Karamadazı; Kr — Kerkenez; Ks — Keskin; Sh — Sarıhacılı; Ss — Satansarı; Su — Sulakyurt; Te — Terlemez; Uk — Üçkapılı; Ya — Yassıağıl; Ba — Bayındır; Yz — Yozgat magmatic association.

the İzmir–Ankara–Erzincan Suture Zone (IAESZ) on the south (e.g., Göncüoğlu et al. 1997a; Bozkurt & Mittwede 2001). The Arabian Plate and the South Anatolian Ophiolite Belt are found in the south of Central Anatolia (e.g., Göncüoğlu et al. 1997a; Bozkurt & Mittwede 2001). The CACC, on the other hand, represents the crustal blocks of the Tauride–Anatolide Platform in between these orogenic belts (e.g., Göncüoğlu et al. 1997a).

The basement units of the CACC are Precambrian–Early Paleozoic metamorphic rocks (Fig. 1), which comprise gneisses and schists, and overlying Late Paleozoic–Mesozoic calc-schists and marbles. These units are suggested as the metamorphosed conjugate members of Precambrian–Mesozoic Tauride units by Göncüoğlu et al. (1993). On these metamorphic rocks, there are Late Jurassic–Upper Cretaceous ophiolitic rocks, which are accepted as the remnants of the İzmir–Ankara–Erzincan Ocean (e.g., Yalınız et al. 2000, Toksoy-Köksal et al. 2009; Göncüoğlu et al. 2010). These ophiolites are generally represented by gabbroic rocks and are of supra-subduction type (e.g., Floyd et al. 1998; Koçak et al. 2005). Kadıoğlu et al. (1998b) additionally reported the existence of ophiolitic gabbro also in the close regions to the CACC, namely to the west of Tuz Lake. There are also intrusive gabbroic rocks in the CACC reported by various authors (e.g., Kadıoğlu & Özsan 1997; Kadıoğlu & Güleç 1996, 1998; Kadıoğlu et al. 2003). Consequently, the existence of both intrusive and ophiolitic gabbro types in the CACC is eventually accepted (e.g., Kadıoğlu & Güleç 2001; Toksoy-Köksal et al. 2010).

Granitoids in the CACC cut the basement and ophiolitic rocks and range from collisional peraluminous and two-mica S-type leucogranites and/or granodiorites (details in Göncüoğlu et al. 1993; Yalınız et al. 1999), to I- and A-type granitic and monzonitic granitoids (details in Göncüoğlu et al. 1993, 1997b; Köksal et al. 2012, 2013). A-type quartz-syenite and foid syenites commonly intrude I-type granitoids but form associations in some places in the CACC (e.g., Göncüoğlu et al. 1997b; Köksal et al. 2004; Deniz & Kadıoğlu 2016).

The succession in Central Anatolia is unconformably overlain by unmetamorphosed Upper Maastrichtian–Lower

Paleocene cover units, Paleocene–Eocene volcanic, volcanoclastic and carbonate rocks, Oligocene–Miocene evaporates, terrestrial clastics, volcanoclastic and volcanic rocks (Göncüoğlu et al. 1993).

Analytical methods

Rocks were crushed and disintegrated into a powder form by using jaw crusher and agate disc mill at the Central Laboratory of Middle East Technical University (METU). Furthermore, whole-rock elemental and radiogenic isotope geochemical analyses from seven samples were conducted at the Central Laboratory of METU (Tables 1 and 2).

Major, trace and rare earth elements (REE) were determined after $LiBO_2/Li_2B_4O_7$ fusion by Perkin Elmer Optima 4300DV ICP-OES and after dilute nitric acid digestion (HNO_3 of 5 %) by Perkin Elmer DRC II ICP-MS. Detection limits of these analyses are 0.01 wt. % for SiO_2, Al_2O_3, MgO, CaO, Na_2O, K_2O, MnO, and TiO_2, 0.04 wt. % for Fe_2O_3, 0.001–0.002 wt. % for P_2O_5 and Cr_2O_3 and 0.10 wt. % for LOI. For trace and REE detection limits are 8 ppm for V, 1 ppm for Ba, 0.5 ppm for Sr, Gd and W, 0.3 ppm for Nd, 0.1 ppm for Cs, Hf, Nb, Rb, Ta, U, Y, Zr, Th, La and Ce, 0.05 ppm for Sm, Dy, Yb, 0.03 ppm for Er, 0.02 ppm for Pr, Eu and Ho, 0.01 ppm for Tb, Tm, Lu. Standard errors were 0.001–0.7 for major elements, 5×10^{-8}–4×10^{-6} for trace elements and 1×10^{-8}–1×10^{-6} for REE.

For radiogenic isotope analyses, Sr was enriched through 2 ml volume BioRad AG50 W-X8 (100–200 mesh) resin by using 2.5 N HCl. REE were collected with 6 N HCl after Sr chromatography, and Nd was separated from other REE in 2 ml HDEHP (bis-ethyexyl phosphate) coated biobeads (BioRad) resin with 0.22 N HCl. Strontium was loaded on single Re filament with Ta-activator and dilute H_3PO_4. Neodymium, on the other hand, was loaded on double filaments with dilute H_3PO_4. $^{86}Sr/^{88}Sr$ ratios were normalized to $^{86}Sr/^{88}Sr = 0.1194$, and NIST SRM 987 standard was measured as $^{87}Sr/^{86}Sr = 0.710244\pm8$ (n=2). $^{143}Nd/^{144}Nd$ ratios were normalized with $^{143}Nd/^{144}Nd = 0.7219$ and La Jolla Nd standard was measured as $^{143}Nd/^{144}Nd = 0.511847\pm5$ (n=2). Isotopic ratios were measured with a Thermo-Fisher Triton TIMS. No bias correction was applied for Sr and Nd analyses. Quality control of the isotope analyses was checked by applying the same procedures to the USGS rock standards. During the period of analyses, the BCR-1 USGS standard gave $^{87}Sr/^{86}Sr = 0.705027\pm12$ (n=3) and AGV-2 USGS standard gave $^{143}Nd/^{144}Nd = 0.512776\pm10$ (n=5). Details of the radiogenic isotope methods are described by Köksal et al. (2017).

Table 1: Whole-rock elemental geochemical data of the intrusive rocks from the Hacımahmutuşağı area.

	HM-1	HM-2	HM-3	HM-4	HM-5	HM-6	HM-7
	GR	LG	GR	LG	GRD	F.GAB	P.GAB
SiO_2 (wt. %)	69.78	74.27	71.06	74.27	68.07	51.80	52.44
TiO_2 (wt. %)	0.33	0.07	0.17	0.10	0.32	0.97	0.48
Al_2O_3 (wt. %)	13.95	11.53	14.93	12.85	16.06	17.95	9.26
$Fe_2O_3^{tot}$ (wt. %)	3.10	0.77	1.92	1.19	4.00	11.01	8.44
MnO (wt. %)	0.058	0.089	0.083	0.059	0.062	0.235	0.146
MgO (wt. %)	1.14	0.14	0.46	0.21	0.95	4.48	13.10
CaO (wt. %)	2.83	0.69	1.80	0.97	4.52	6.46	13.99
Na_2O (wt. %)	2.72	3.71	3.64	3.26	3.64	3.37	1.28
K_2O (wt. %)	4.34	5.26	4.58	4.82	1.73	2.53	0.96
P_2O_5 (wt. %)	0.0008	0.0002	0.0004	0.0002	0.0015	0.0018	0.0008
LOI (wt. %)	1.4	1.3	1.1	1.1	1.3	1.3	0.8
SUM (wt. %)	99.64	97.82	99.75	98.83	100.65	100.10	100.90
Ba (mg/kg)	620	166	440	182	580	730	470
Cs (mg/kg)	9.1	8.2	6.5	27.8	1.23	3.1	0.74
Ga (mg/kg)	16.5	15.1	15.7	14	18.6	22.9	10.1
Hf (mg/kg)	2.31	2.91	2.38	2.48	0.82	1.24	0.92
Nb (mg/kg)	8.7	26.3	10.1	19.2	6.1	11.7	2.25
Rb (mg/kg)	180	431	254	331	55	106	26.8
Sr (mg/kg)	134	34	110	45	359	256	238
Ta (mg/kg)	0.94	3.94	1.15	3.33	0.41	0.72	0.17
Th (mg/kg)	17.8	24.2	24.2	33	9.1	5.69	3.73
U (mg/kg)	4	10.1	5.4	9.7	0.87	1.46	1.02
V (mg/kg)	39	5.51	25.6	9.9	42	276	230
Zr (mg/kg)	69	65	64	60	25	29	23
Y (mg/kg)	17.9	33.2	20.1	22.8	8.8	28.9	12.1
La (mg/kg)	26.4	13.9	17	18.2	29.2	8.05	10.6
Ce (mg/kg)	51	28.3	33.3	33.7	53	22.1	19.8
Pr (mg/kg)	5.69	3.17	3.16	3.5	5.29	3.41	2.33
Nd (mg/kg)	18.6	11.2	10.5	11.5	17.1	15.6	9.15
Sm (mg/kg)	3.71	3.44	2.36	2.52	2.76	4.62	2.43
Eu (mg/kg)	0.72	0.17	0.46	0.24	0.96	1.23	0.68
Gd (mg/kg)	3.27	4.04	2.41	2.62	2.18	4.79	2.45
Tb (mg/kg)	0.5	0.81	0.42	0.48	0.29	0.79	0.36
Dy (mg/kg)	2.96	5.31	2.64	3.17	1.58	5.02	2.14
Ho (mg/kg)	0.58	1.11	0.58	0.66	0.28	1.02	0.41
Er (mg/kg)	1.88	3.38	1.85	2.36	0.82	3.05	1.21
Tm (mg/kg)	0.28	0.51	0.31	0.37	0.12	0.42	0.16
Yb (mg/kg)	1.87	3.59	2.24	2.81	0.82	2.68	1.02
Lu (mg/kg)	0.27	0.52	0.36	0.45	0.13	0.4	0.15
Pb (mg/kg)	23	49	39	38	20	15.3	10.2
$(Eu/Eu^*)_N$	0.63	0.14	0.59	0.28	1.19	0.80	0.85
$(La/Yb)_N$	9.59	2.63	5.16	4.40	24.19	2.04	7.06
A/CNK	0.97	0.80	1.01	0.96	1.15	1.03	0.42
Mg-no	27	15	20	15	19	29	61

Note: $Fe_2O_3^{tot}$=total Fe; LOI=loss on ignition; $(Eu/Eu^*)_N=(Eu_N)/\sqrt{(Sm_N\times Gd_N)}$; Eu_N, Sm_N, Gd_N, La_N and Yb_N values are normalised to chondrite (McDonough & Sun 1995); A/CNK= molar$[Al_2O_3/(CaO+Na_2O+K_2O)]$; Mg-no=100×Mg/(Mg+Fe). GR: granite; GRD: granodiorite; LG: leucogranite; F.GAB: fine-grained gabbro; P.GAB: pegmatitic gabbro.

Field characteristics

Metamorphic rocks form the basement units of the Hacımahmutuşağı area (Fig. 2) (e.g., Göncüoğlu et al. 1993), and these units are contemporary with the Kalkanlıdağ and Tamadağ formations (e.g., Seymen 1981) or Gümüşler and Aşıgediği formations (e.g., Göncüoğlu 1986; Göncüoğlu et al. 1993) in the other parts of Central Anatolia. Gneisses, oldest rock units of the CACC (i.e., Kalkanlıdağ or Gümüşler

formations), crop out in the middle-north part of the Hacımahmutuşağı area. Marbles (i.e., Tamadağ or Aşıgediği formations) transitionally overlay gneisses and generally dip to the southeast. Well defined contact metamorphism between the basement rocks and the intrusive rocks are observed in the study area.

Gabbroic rocks in the study area are dark coloured and represented by two types as pegmatitic gabbros, including large amphibole crystals, and fine-crystalline gabbros occupying larger areas than the pegmatitic ones. The contact zones of gabbros and the metamorphic rocks are concealed by recent cover units in the study area, but in the north-eastern part of the study area some gabbro blocks have fallen over the marbles. Thus, these gabbros were initially suggested by Köksal (1992) and Köksal et al. (2001) as rocks belonging to the allochthonous ophiolitic units observed in various parts of the CACC (e.g., Sarıkaraman: Yalınız et al. 2000; Ekecikdağ: Göncüoğlu & Türeli 1994; Köksal et al. 2017). However, the geochemical findings presented in this study show that the gabbros and the granitoids have similar petrological features. Therefore, the field relations of gabbros and marble should be resulted from the subsequent tectonic events. Similar gabbroic rocks observed in the Hacımahmutuşağı area were initially documented in the NW of the study area in the Ağaçören (e.g., Güleç et al. 1996; Kadıoğlu et al. 1998a, 2003) and SE of the study area in the Ekecikdağ (e.g., Göncüoğlu & Türeli 1994) areas. Kadıoğlu et al. (2003) indicated that the granitoids and the gabbros in the Ağaçören area are coeval and gabbro blocks in the area belong to the large intrusive bodies emplaced 1.55 km deep based on the magnetic modelling studies.

The granitoids in the Hacımahmutuşağı area are differentiated into two groups: granite–granodiorite and leucogranite (Fig. 3). Granite–granodiorite is the main intrusive phase in the area (Figs. 2, 3a,b,c). Granite–granodiorite is characterized by large feldspar crystals and visible quartz and mafic mineral content (Fig. 3c). Leucogranite, on the other hand, is a relatively younger phase with white colour and very little mafic mineral content (Fig. 3d). Leucogranite cuts both granite–granodiorite and host rock marble (Fig. 2).

Table 2: Whole-rock Sr–Nd isotopic data of the intrusive rocks from the Hacımahmutuşağı area.

		$^{87}Sr/^{86}Sr$	$^{87}Sr/^{86}Sr_{(i)}$	$^{143}Nd/^{144}Nd$	$^{143}Nd/^{144}Nd_{(i)}$	$\varepsilon Nd_{(i)}$
HM-1	GR	0.716092±15	0.711672	0.512096±4	0.512033	−9.8
HM-2	LG	0.749279±15	0.707566	0.512326±4	0.512229	−6.0
HM-3	GR	0.716779±12	0.709181	0.512285±3	0.512214	−6.3
HM-4	LG	0.734712±18	0.710508	0.512263±3	0.512194	−6.7
HM-5	GRD	0.710307±7	0.709803	0.512202±2	0.512151	−7.5
HM-6	F.GAB	0.710504±6	0.709141	0.512302±2	0.512208	−6.4
HM-7	P. GAB	0.708530±8	0.708159	0.512364±3	0.512280	−5.0

Note: Rb, Sr, Nd and Sm concentrations are taken from Table 1. Initial isotopic ratios are calculated for t=80 Ma. GR: granite, GRD: granodiorite, LG: leucogranite, F.GAB: fine-grained gabbro, P.GAB: pegmatitic gabbro.

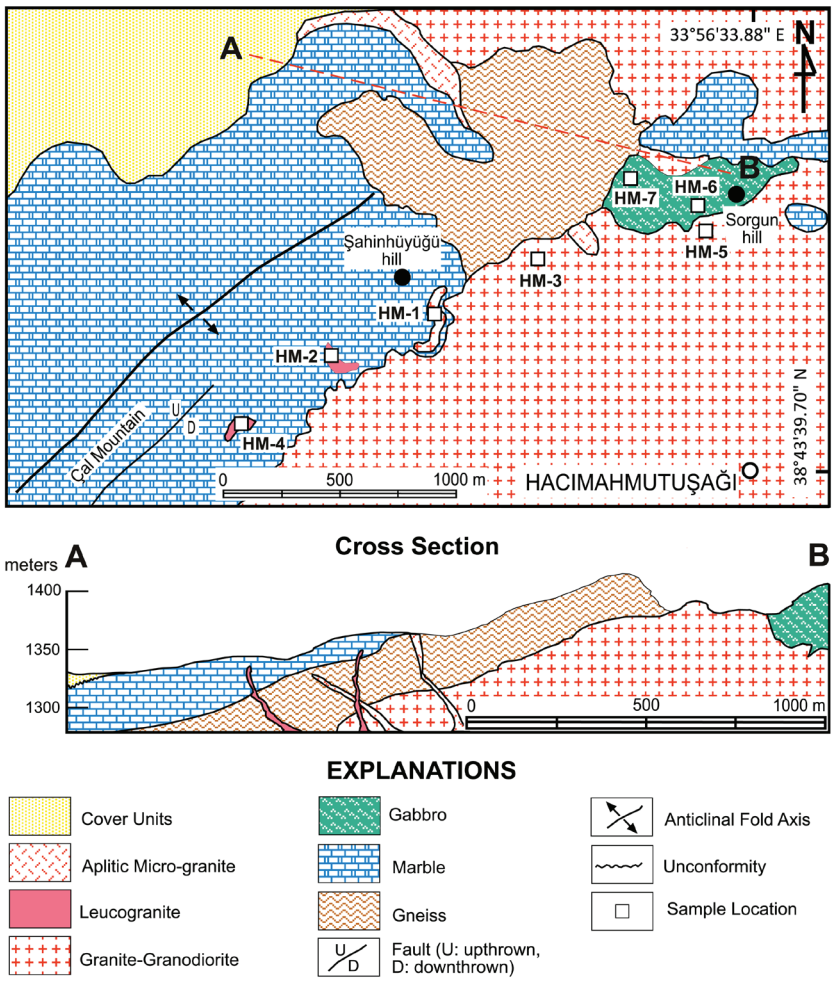

Fig. 2. Geological map and cross section of the study area (GPS coordinates of samples are: HM-1: 38°43’57.38” N, 33°55’43.02” E; HM-2: 38°43’51.37” N, 33°55’25.08” E; HM-3: 38°44’4.18” N, 33°56’0.68” E; HM-4: 38°43’42.46” N, 33°55’10.78” E; HM-5: 38°44’7.65” N, 33°56’31.87” E; HM-6: 38°44’11.25” N, 33°56’28.89” E; HM-7: 38°44’14.90” N, 33°56’18.04” E).

Granitoids in the nearby areas were investigated in detail in previous works; Ağaçören granitoids (e.g., Kadıoğlu et al. 2003; Köksal et al. 2012) and Ekecikdağ granitoids (e.g., Göncüoğlu & Türeli 1994; Toksoy-Köksal, 2016). Granite–granodiorite in the study, considering the geological and petrological features, resembles amphibole-biotite granite in

the Ağaçören area (Kadıoğlu et al. 2003) and/or Borucu granitoid in the Ekecikdağ area, leucogranite on the other hand is similar to the Kalebalta leucogranite in the Ekecikdağ area (Göncüoğlu & Türeli 1994). Moreover, there are widespread aplitic micro-granite dykes reaching up to hundreds of metres long, cutting the gneisses and granitoids and representing the youngest intrusive phase in the study area. In this area, metamorphic rocks are found as roof-pendants on the granitoids (Fig. 2). There are dykes of granite–granodiorite and leucogranite along the contacts and inside the marble units. The wollastonite hornfelses observed along the granitoid–marble contact indicate intrusive features of the granitoids in the studied area. Gabbros, mafic microgranular enclaves and granitoids have generally sinuous contacts in the study area (Fig. 3b). Neogene cover units, represented by fluvial and lacustrine deposits, unconformably overlay older units in the area (Fig. 2).

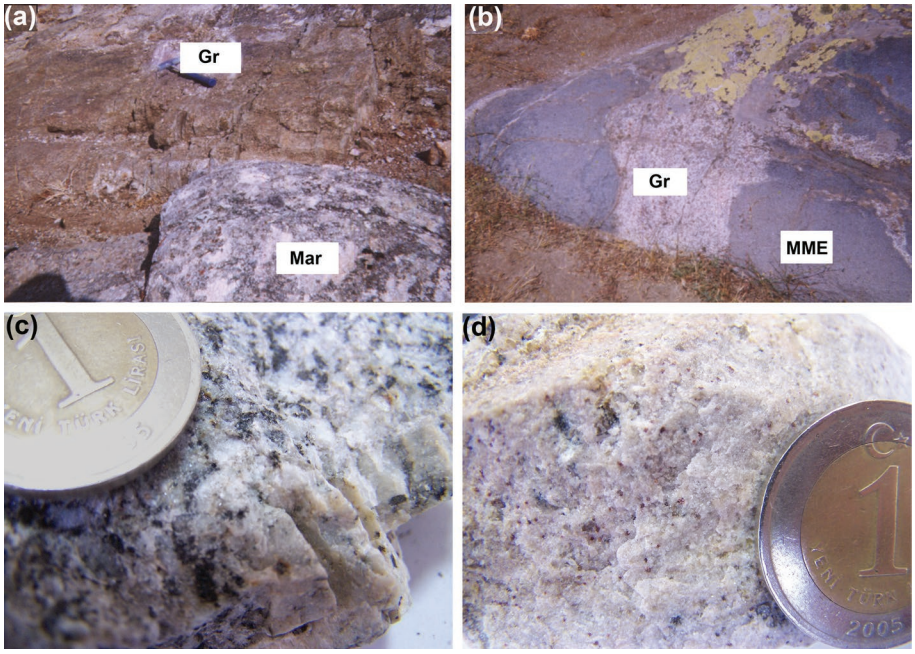

Fig. 3. Field views of the studied intrusives and their contact relationships: **a** — granite–granodiorite (Gr) and marble (Mar); **b** — photograph showing granite-granodiorite (Gr) and large mafic microgranular enclave (MME); **c** — granite–granodiorite close-up view; **d** — leucogranite close-up view.

Results

Petrography

Gneisses have intermediate to highly developed gneissic texture with quartz, feldspar and garnet crystals in between biotite, sillimanite and cordierite rich bands. The main contact metamorphic phase is cordierite and related to the intrusion of the aplitic micro-granite. Marbles with granoblastic and massive texture show large calcite crystals along the contacts of the intrusive rocks.

Pegmatitic gabbros are represented by abundant large hornblend crystals. The main minerals are hornblend, plagioclase (andesine and/or labradorite), clinopyroxene (diopside) and opaque minerals; secondary minerals are chlorite and epidote (Fig. 4a,b). Fine-grained gabbros are composed of plagioclase, hornblend, biotite as main mineral phases and chlorite as secondary, opaque minerals and apatite as accessory minerals (Fig. 4c,d,e). In both gabbro types, there are extensive uralitizations, where hornblendes are partly preserved along the rims of the clinopyroxenes (e.g., Fig. 4a). These gabbros can be interpreted as uralitic gabbros although this is not the case for the whole gabbroic intrusions. Moreover, along the granitoid–gabbro contact, primary hornblend in the gabbroic part was generally replaced by actinolite and chlorite due to the heat transfer and chemical interaction between gabbro and semi-solid granitoid (Fig. 4d,e,f). Chilled margins along these contacts are also observed in the study area (Fig. 4f).

Granite–granodiorites are characterized by phaneritic texture and greyish colour with 15–25 % mafic mineral content and widespread argillitization and sericitization. Quartz, orthoclase, plagioclase, hornblend and biotite are the major minerals, with minor amounts of opaque minerals, zircon and secondary muscovite (Fig. 4g). Leucogranites have white colour, medium grained texture and scarce mafic content (ca. 5–10 %) with quartz, orthoclase and albitic plagioclase as the main mineral phases, and chloritized biotite, hornblend, epidote, apatite and opaque minerals as accessory minerals (Fig. 4h). Micrographic and myrmekitic textures are also well-developed in the studied leucogranites. Aplitic micro-granite dykes on the other hand are light coloured rocks with fine grained, holocrystalline and microgranular texture. These dykes have quartz and orthoclase — extensively argillitized and sericitized — as major, plagioclase as minor, and garnet, tourmaline and opaque minerals as accessory minerals. Wollastonite hornfelses with wollastonite, diopside and epidote minerals are the contact metamorphism products observed in the study area.

Major and trace element geochemistry

Geochemical data from the whole-rock elemental analyses studied are given in Table 1. In the Kadıoğlu et al. (2003) study covering the Hacımahmutuşağı area five gabbro samples fall into the boundaries of the study area of the present research. The data from these five gabbro samples, which were documented by Kadıoğlu et al. (2003), are specified as

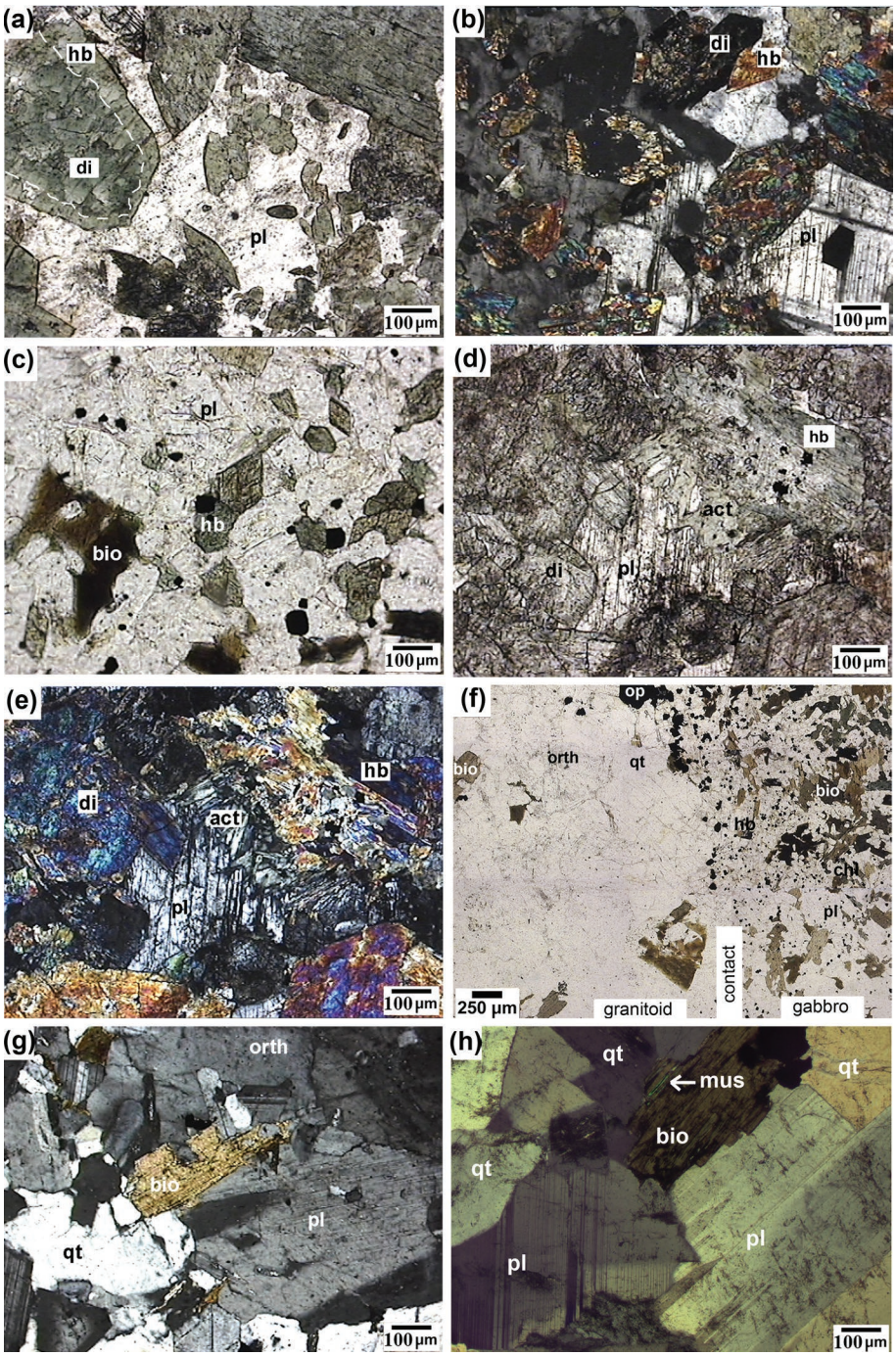

Fig. 4. Photomicrographs of the gabbros and granitoids: **a, b** — pegmatitic gabbro, plane polarized light (a), crossed polars (b); **c, d, e** — fine crystalline gabbro, plane polarized light (c, d), crossed polars (e); **f** — microscopic view from the contact of granitoid and gabbro, plane polarized light. **g** — granite–granodiorite, crossed polars; **h** — leucogranite, crossed polars. qt: quartz, orth: orthoclase, bio: biotite, pl: plagioclase, hb: hornblend, mus: muscovite, op: opaque minerals, chl: chlorite, di: diopside, act: actinolite.

gabbro(2) in the geochemical diagrams and are evaluated along with the new geochemical data presented in Table 1 for better assessment.

On the Na_2O+K_2O vs. SiO_2 diagram of Cox et al. (1979), HM-7 (pegmatitic gabbro) and the gabbro samples from Kadıoğlu et al. (2003), plot into the sub-alkaline area while HM-6 (fine-grained gabbro) falls in the alkaline area (Fig. 5a). In the same diagram, the studied granitic rocks, namely granodiorite/granite, show transition from granodiorite to alkali granite, and these samples which cannot be exactly distinguished based on field and petrographic observations, are identified by using this classification (Fig. 5a). Excess silica contents of the gabbro samples concerned in this study (Table 1; Fig. 5a) infer their geochemical compositions are akin to diorites. However, based on the nomenclature revealed by Na_2O+K_2O vs. SiO_2 diagram (Fig. 5a) and to be consistent with the existing literature (e.g., Kadıoğlu et al., 2003, 2006; Kadıoğlu and Güleç, 1998, 2001; Güleç and Kadıoğlu, 1998) the mafic intrusive rocks in the present research are named and evaluated as "gabbro".

Granite and leucogranite show transition from calc–alkalic to alkali–calcic field, while granodiorite is in the calcic part on the Na_2O+K_2O-CaO vs. SiO_2 diagram (Frost et al. 2001) (Fig. 5b). LOI values of the rock samples (Table 1) show less than 1.5 % inferring secondary events like argillitization and sericitizion are not very effective in evaluating geochemistry. However, it is plausible to describe the samples as sub-alkaline by using trace elements, which are less affected by alteration (Fig. 5c).

On the AFM diagram (Irvine & Baragar 1971), granitoids and fine-grained gabbro (HM-6) display calc–alkaline character, whereas pegmatitic gabbro and gabbro(2) show transition from calc–alkaline to tholeiitic (Fig. 5d). Based on the A/CNK values granitoids in the area can be described as metaluminous except a granodiorite sample showing weak peraluminous character (Table 1). In addition, regarding the magnesium numbers, leucogranite have the lowest, and pegmatitic gabbro has the highest Mg-no (Table 1) among the rock samples analysed.

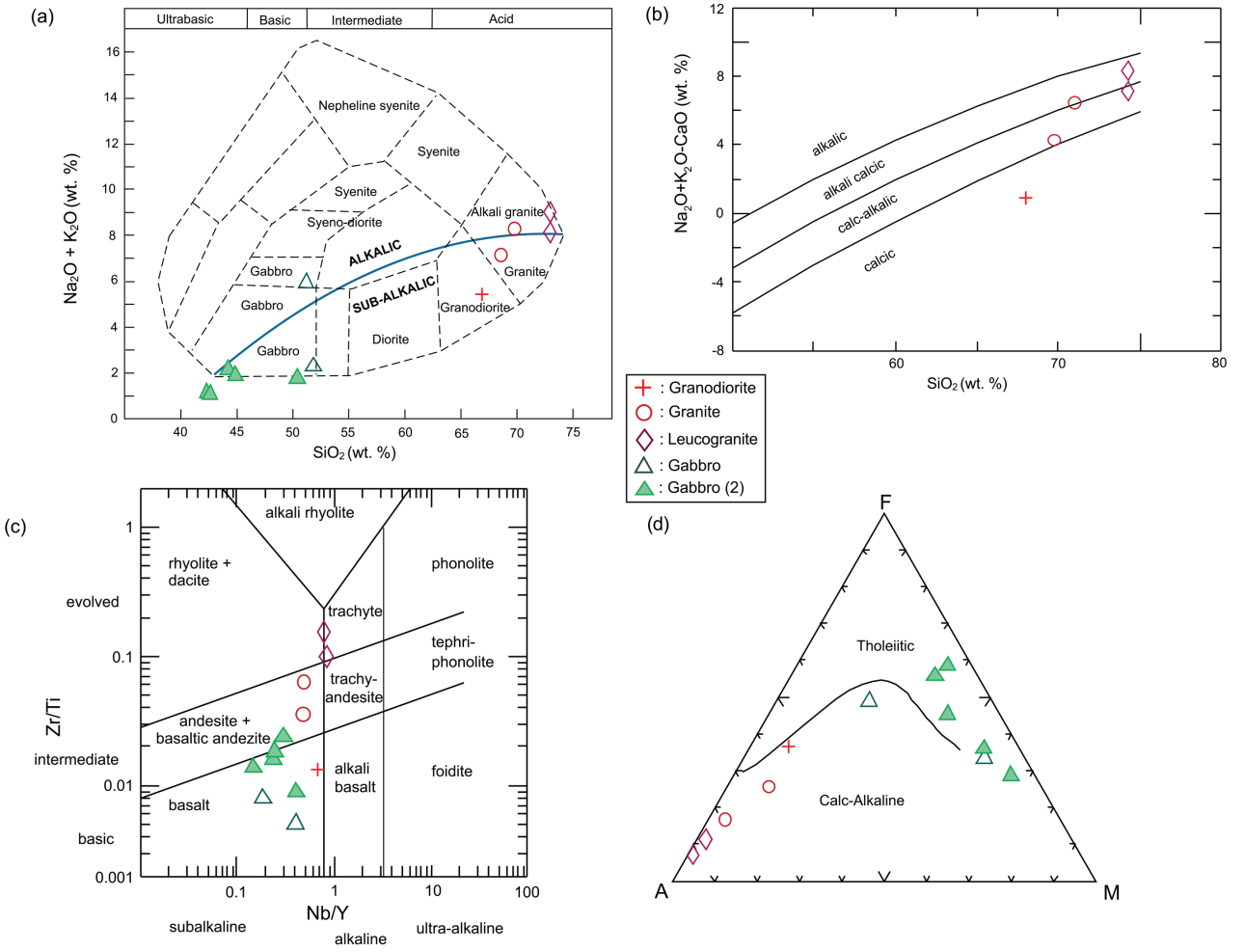

Fig. 5. Intrusive rocks in the study area: **a** — nomenclature based on the Na_2O+K_2O vs. SiO_2 diagram (Cox et al. 1979); **b** — classification based on the Na_2O+K_2O-CaO vs. SiO_2 diagram (Frost et al. 2001); **c** — Zr/Ti–Nb/Y diagram (Pearce 1996); **d** — A–F–M diagram (Irvine & Baragar 1971).

When Harker diagrams plotted against SiO_2 are evaluated it is difficult to mention a genetic relationship between granitoids and gabbros. The scatter of the gabbro samples and a gap between the gabbros and granitoids, also considering the fewness of the analysed samples, there are not enough findings to suppose a trend inferring fractionation from mafic to felsic rocks in the area (Fig. 6). Although it is possible to deduce that leucogranite has similar but less evolved/enriched source than granite, granodiorite exhibits the most depleted source among the granitoids (Fig. 6). The similar situation stands out in the trace elements vs. SiO_2 diagrams (Fig. 7). Variation in the genetic characteristics within the granitic rocks, especially for Rb, Ba, Sr, Nb, U, Y and V elements, is remarkable (Fig. 7). Granodiorite displays depletion in Nb, Rb, Th, U, Zr, and Pb with respect to granite and leucogranite. In contrast, gabbro samples exhibit less crustal contribution (e.g., U, Pb, and Rb) than granitoids and cluster in different areas than the granitoids in trace element vs. SiO_2 diagrams (Fig. 7).

On the multi-element diagram normalized to primitive mantle (Sun & McDonough 1989) granitoids and gabbros show similar trends, where gabbros illustrate relatively lower Th, La, Ce, Pb and higher Ti contents. Furthermore, depletion of Rb, Nb and Ta is significant in pegmatitic gabbro. Leucogranites presenting Ba, P, Eu and Ti depletion with Pb, K, U and Th enrichment differ from other rocks with their higher crustal contribution/effect in their source (Fig. 8a). Nb–Ta depletion observed in the Figure 8a may be related with the earlier subduction component inherited in the source region, but it is also characteristic for the continental crust (Kelemen et al. 1993). Chondrite-normalized REE patterns (Sun & McDonough 1989) infer LREE are more enriched than HREE in all samples, while gabbros have lower LREE contents than granitoids (Fig. 8b). La/Yb fractionation is the highest in granodiorite ($[La/Yb]_N$=24.19), moderate to high in granite ($[La/Yb]_N$=5.16–9.59), and lower and limited in leucogranite ($[La/Yb]_N$=2,63–4,40). Data from gabbros, on the other hand, are fairly scattered ($[La/Yb]_N$=2.04–7.06). Negative Eu anomalies of granite ($[Eu/Eu^*]_N$=0.59–0.63) and leucogranite ($[Eu/Eu^*]_N$=0.14–0.28) put forward plagioclase fractionation. Conversely positive Eu anomaly of granodiorite ($[Eu/Eu^*]_N$=1.19) suggests plagioclase fractionation is not pronounced, but amphibole fractionation should

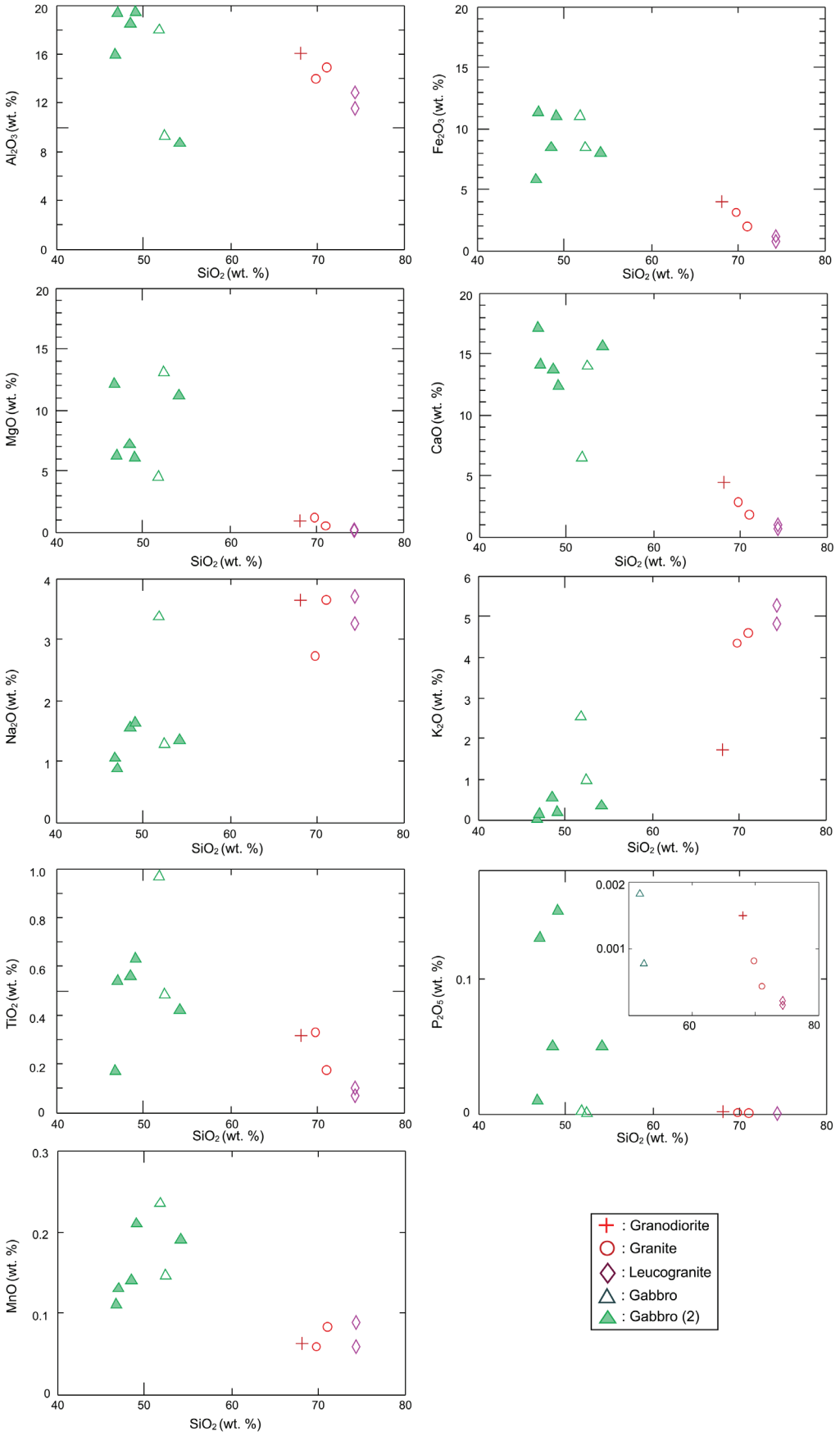

Fig. 6. Harker diagrams of the intrusive rocks (SiO_2 vs. major elements).

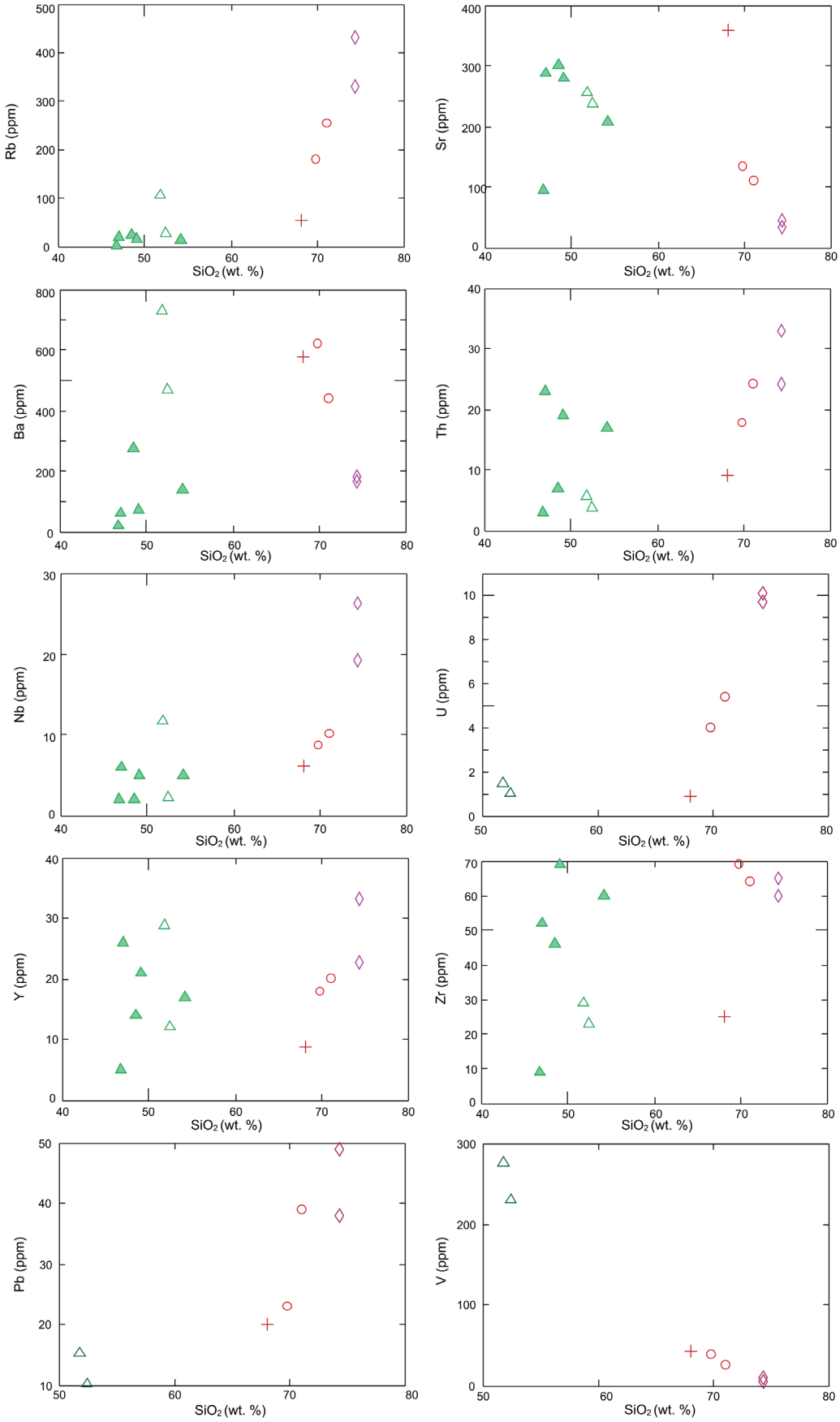

Fig. 7. Harker diagrams of the intrusive rocks (SiO_2 vs. trace elements). Symbols are from the Figure 6.

be the case concerning the bowl shape pattern of HREE (Fig. 8b). Moreover for the gabbro samples showing weak Eu anomaly ($[Eu/Eu^*]_N$=0.80–0.85) plagioclase fractionation does not seem prevalent.

Tectonic discrimination diagrams (Fig. 9a,b) indicate that granitoids show syn-collisional character. However, a granodiorite sample plotted in volcanic arc field in Rb vs. Yb+Ta diagram (Pearce et al. 1984) (Fig. 9a) shows transition from syn-collisional to late and post-collisional stage granitoids in Rb/30–Hf–Tax3 diagram (Harris et al. 1986) (Fig. 9b). Nb/Yb vs. Th/Yb diagram (Fig. 9c) points to enriched source for all intrusive rocks investigated with a large recycled crustal component (Pearce 2008).

Considering the geochemical data along with the petrographic examinations (mafic mineral contents of granite/granodiorite and leucogranite) we can suggest that granitoids among themselves were subjected to different levels of fractionation and/or crustal contamination processes. Since there are no age data from each granitoid type available exact description of the genetic relationships is not possible. However, in the nearby area (Ekecikdağ) similar leucogranites are reported to be younger than the granite/granodiorites based on geochronological data (Toksoy-Köksal 2019). Thus, granodiorite may represent the first and leucogranite is the last granitic phase in the Hacımahmutuşağı area.

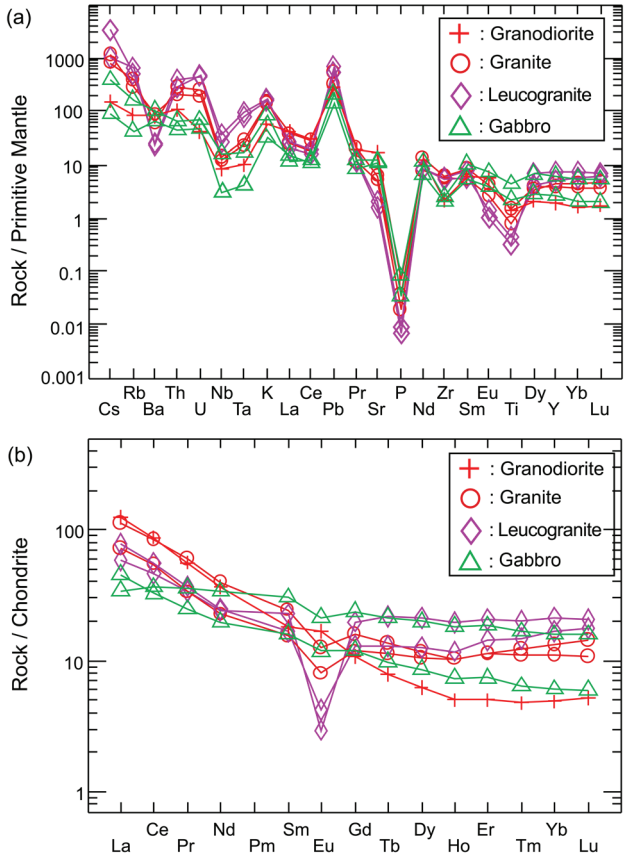

Fig. 8. a — Primitive mantle-normalized (Sun & McDonough 1989) multi-element spider diagram; **b** — chondrite-normalized (Sun & McDonough 1989) REE diagram.

Sr–Nd isotope geochemistry

Initial Sr and Nd isotope ratios are calculated for 80 Ma (Köksal et al. 2012) (Table 2; Fig. 10). Kadıoğlu et al. (2003) reported apparent $^{40}Ar/^{39}Ar$ ages for gabbro samples in the Hacımahmutuşağı area as 78.0±0.3 Ma to 78.8±1.0 Ma; and 77.7±0.3 Ma for a granite sample close to southeast of the study area. However similar granitoids in the Ağaçören region near the Hacımahmutuşağı area yield older U–Pb zircon ages (Köksal et al. 2012), therefore these Ar–Ar ages are assumed to be the cooling age and 80 Ma is suggested for the intrusive rocks in the study area.

Initial strontium isotope data for granitoids are in the $^{87}Sr/^{86}Sr_{(i)}$=0.707566–0.711672 interval, but there is no significant variation in between leucogranite, granite and granodiorite samples considering the initial Sr isotope ratios (Table 2). Güleç (1994) also reported $^{87}Sr/^{86}Sr_{(i)}$=0.708616 (n=3) data from the Ağaçören granitoid on the NW of the study area. A similar case is valid for the gabbros where fine-grained gabbro yields $^{87}Sr/^{86}Sr_{(i)}$=0.709141 and pegmatitic gabbro gives $^{87}Sr/^{86}Sr_{(i)}$=0.708159 values; and these data are comparable to those of the granitoids (Table 2; Fig. 10). Furthermore granite-granodiorite shows a larger range of initial Nd isotope data ($^{143}Nd/^{144}Nd_{(i)}$=0.512033–0.512214; $\varepsilon Nd_{(i)}$=−6.3 to −9.8), than leucogranite displaying $^{143}Nd/^{144}Nd_{(i)}$=0.512194– 0.512229; $\varepsilon Nd_{(i)}$=−6.0 to −6.7 values (Table 2). Initial $^{143}Nd/^{144}Nd$ isotope ratios for fine-grained gabbro and pegmatitic gabbro are 0.512208 ($\varepsilon Nd_{(i)}$=−6.4) and 0.512280 ($\varepsilon Nd_{(i)}$=−5.0), respectively (Table 2). Neodymium isotope data of gabbros also reflect that they are comparable to the granitoids isotopically. This situation is rather different from the expected isotopic ratios where gabbros display higher $^{143}Nd/^{144}Nd$ and lower $^{87}Sr/^{86}Sr$ ratios than granitoids elsewhere (e.g., Miller et al. 2011). While the HM-1 granite sample has the most crustal contribution among the intrusive samples, the HM-7 pegmatitic gabbro sample has the least initial Nd isotope data. Collectively Sr and Nd isotope data yielding high $^{87}Sr/^{86}Sr_{(i)}$ ratios, 0.7076 to 0.7117, and low $\varepsilon Nd_{(i)}$ values, −5.0 to −9.8, indicate that the intrusive rocks concerned have the enriched source with high crustal input instead of depleted mantle source (Fig. 10).

Discussion

CACC intrusive rocks have been the subject of various studies, but their petrology is not sufficiently clear because of their complex geodynamic environment. In this manner investigation of the Cretaceous intrusive rocks of the CACC is important for understanding the Alpine orogenesis. The Hacımahmutuşağı area in this way is one of the unique areas in Central Anatolia for studying the petrogenesis of these rocks and their relationships. The geochemical data presented in this study infer that both rock types are formed in similar tectonic environments. The cutting relationship between granitoid and gabbro is revealed by geological and petrographical

observations. The chilled margin along the contact zones between granitoids and gabbros may imply rapid cooling along the zone of coeval granitoid and hotter gabbroic body. Contemporaneous evolution of granitoid and gabbro may ascribe heterogeneity in the source region. However, intrusion of gabbro into the granitoid is the case, which cannot be completely ruled out. Granitoid evolution might have ceased when enriched partial melts could no longer form and succeeding magmatism integrated with less fertile restite compositions, generating gabbros but with a noticeable compositional gap (e.g., Meade et al. 2014), as detected in the Harker diagrams of the intrusive rocks in the study area. In that case gabbro intrusion might be relatively younger (e.g., 1 or 2 Ma) than granitoid.

On the initial εNd vs. $^{87}Sr/^{86}Sr$ diagram isotopic characters of granitoids and gabbros from the Hacımahtuşağı area are similar and comparable to that of I- (and/or A-) type hybrid Central Anatolian granitoids (Fig. 10). Conversely, initial Sr and Nd isotope data of gabbros (Fig. 10) are very different from the ophiolitic rocks, including gabbros, in the south-east of the study area in the Ekecikdağ region (Köksal et al. 2017). Hacımahmutuşağı gabbros have enriched source, i.e. crust dominated, in contrast to the Ekecikdağ ophiolitic rocks. This interpretation supports the idea of existence of both intrusive and ophiolitic gabbros within the western part of the CACC (e.g., Toksoy-Köksal et al. 2010).

Granitic rocks in the study area are similar to the other I-type granitoids in the CACC by their geological, petrographical and geochemical characteristics while gabbros resemble intrusive gabbroic rocks in the CACC.

There are several approaches to explain the evolution mechanisms of the CACC granitoids and these can be summarized as two main views on the evolution of the granitic rocks in the CACC: (1) they are related to the Andean-type magmatism in the region; (2) they are products of collisional to post-collisional regimes. The first view is proposed by Görür et al. (1984), who argued for subduction of oceanic lithosphere of the Inner Tauride Ocean under the CACC during the Paleocene-Early Eocene times yielding volcanic arc granitoids. Similarly, Kadıoğlu et al. (2006) suggested that the CACC granitoids were formed from partial melting of metasomatized lithospheric mantle rocks combined with assimilation, fractional crystallization and mingling-mixing processes due to the collision of the leading edge of the Tauride platform with a trench within the Inner Tauride Ocean (a Neo-Tethyan seaway) followed by partial subduction, slab break-off and asthenospheric upwelling. Kadıoğlu et al. (2006) subdivided the CACC granitoids into a granite supersuite showing granitic to granodioritic composition, monzonite supersuite having quartz monzonite to monzonite composition, and syenite supersuite, which is represented by

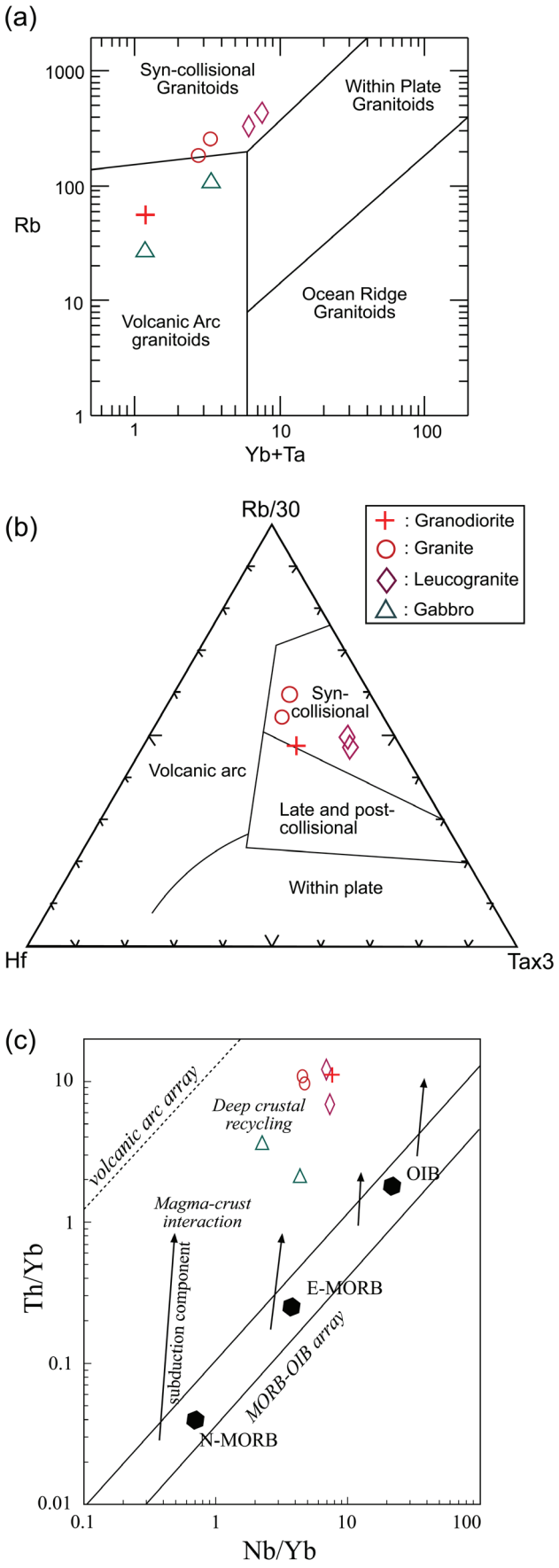

Fig. 9. Tectonic discrimination diagrams of the studied intrusive rocks: **a** — Rb vs. Yb+Ta diagram (Pearce et al. 1984); **b** — Rb/30 –Hf–Tax3 diagram Harris et al. (1986); **c** — Th/Yb vs. Nb/Yb diagram (Pearce 2008).

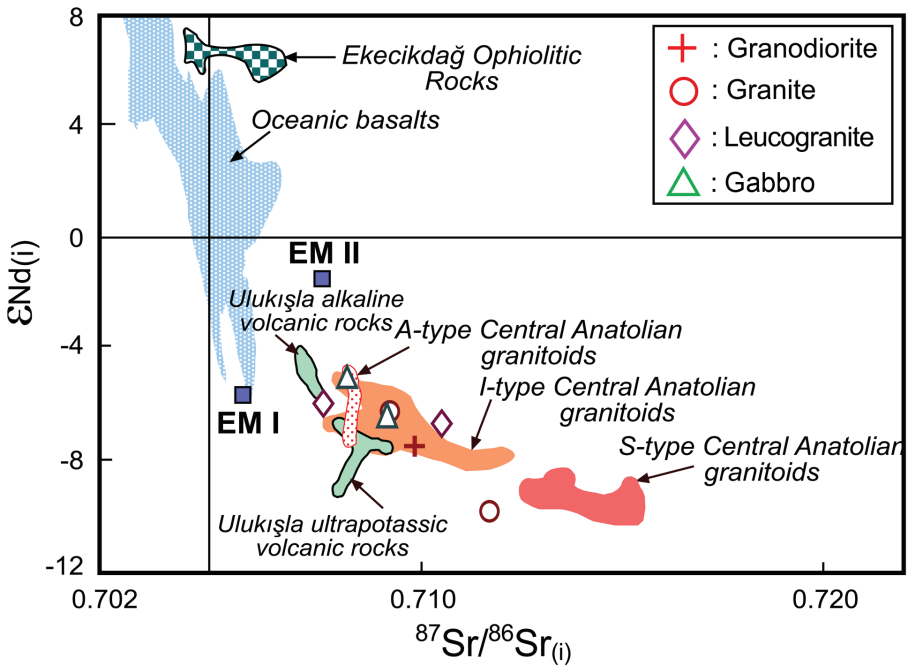

Fig. 10. Initial εNd vs. $^{87}Sr/^{86}Sr_{(i)}$ diagram of the intrusive rocks in the Hacımahmutuşağı area. Areas for comparison: Ekecikdağ ophiolitic rocks (Köksal et al. 2017); S-, I- and A-type Central Anatolian granitoids (Köksal & Göncüoğlu 2008 and references therein); Ulukışla alkaline volcanic rocks (Alpaslan et al. 2004); Ulukışla ultrapotassic volcanic rocks (Alpaslan et al. 2006). Mantle components: EM (enriched mantle) and oceanic basalts are from Zindler & Hart (1986) and Hart (1988).

quartz syenite, syenite, and nepheline- and pseudoleucite-bearing alkali rocks. Kadıoğlu et al. (2006) thought that the derivation of these granitoids is related to subduction instead of collision, yielding a subduction-modified and metasomatized mantle source for granite and monzonite supersuites, and enriched mantle source with considerable crustal contribution for the syenite supersuite magmas. Güleç & Kadıoğlu (1998) suggested the involvement of upper crustal and subduction-modified upper mantle-derived sources with an isotope signature of MORB in the petrogenesis of I-type Ağaçören granitoids to the NW of the study area by using Sr-isotopic data. Mafic microgranular enclaves found in the granitoids provide evidence for magma mingling (Güleç & Kadıoğlu 1998). Moreover, Kadıoğlu et al. (2003) suggested that the evolution of the granitoids and gabbros in a region, covering Hacımahmutuşağı area, are related to the Andean-style magmatic arc, inferring the existence of Inner-Tauride Ocean between the CACC and the Tauride carbonate platform. They further advocated that a subduction zone dipping away from the Tauride platform consumed the floor of the Inner-Tauride ocean basin and resulted in the emplacement of its remnant oceanic crust onto the platform edge, and this subduction zone within the Inner-Tauride ocean basin that produced a magmatic arc along the western margin of the CACC.

The second group, on the other hand, think that during the closure of the northern branch of the Alpine Neotethyan Ocean, ophiolitic rocks overthrusting the CACC basement rocks resulted in crustal thickening followed by thermal relaxation in Central Anatolia. The results of the present study favour the collisional to post-collisional nature for the intrusive rocks in the Hacımahmutuşağı area instead of Andean-style magmatic arc origin.

The collision and subsequent periods caused evolution of collisional to post-collisional granitoids in the region (e.g., Göncüoğlu et al. 1993, 1997b; Yalınız et al. 1999; Boztuğ et al. 2007, 2009; İlbeyli et al. 2004; Köksal et al. 2012, 2013). The second assessment fundamentally disagrees with the existence of the Inner Tauride Ocean, because the proposed place for the Inner Tauride Suture is buried under the Ulukışla Basin (e.g., Robertson et al. 2009), one of the large sedimentary basins in Central Anatolia like Kızılırmak and Sivas, which were formed by thermal relaxation and extensional regime in Upper Maastrichtian–Paleocene (Göncüoğlu et al. 1993; Dirik et al. 1999; Alpaslan et al. 2004; van Hinsbergen et al. 2016). A similar scenario was reported from the Variscan Belt of Europe where evolution of the granitoids are explained as related to the post-collisional restoration and re-equilibration of a thickened continental lithosphere, through delamination and/or erosion of its mantle root and erosion combined with exhumation in a following extensional regime (e.g., Bussy et al. 2000).

Köksal & Göncüoğlu (2008) and Köksal et al. (2004, 2012) suggested that the evolution of the Cretaceous CACC granitoids can be subdivided into three main phases: namely collisional crustal S- and I-type granites-granodiorites of 85–80 Ma, post-collisional A-type syenites and the I-type granitoids, mainly monzonites, formed ca. 75 Ma, and later (i.e. 74 Ma and/or younger) alkaline intrusives, mainly syenites and foid-syenites, and volcanic rocks related to the post-collisional extension in the CACC.

Examples of first group are the Üçkapılı Granitoid (Göncüoğlu 1986), Behrekdağ batholite (İlbeyli et al. 2004) and Danacıobası Granitoid (Boztuğ et al. 2007) (Fig. 1). These granitoids are calc–alkaline rocks associated with thermal influx related to the crustal thickening and coeval with the regional metamorphism (e.g., Göncüoğlu 1986; Whitney et al. 2003). This crustal thickening is claimed to be caused by collision of an ensimatic island arc in the İzmir–Ankara–Erzincan Ocean and the CACC basement rocks in Turonian–Coniacian (e.g., Göncüoğlu 1986). The granitoids in the Hacımahmutuşağı area are probably members of this group of rocks.

Second period granitoids are characterized by Cefalıkdağ quartz-monzonite (Kadıoğlu et al. 2006), Baranadağ quartz-monzonite (Köksal et al. 2004; İlbeyli et al. 2004; Boztuğ et al. 2007), Terlemez quartz-monzonite (Yalınız et al. 1999) and other monzonitic rocks exposed in different parts of the CACC (Fig. 1). These Campanian monzonitic rocks are described as sub-alkaline-transitional (e.g., İlbeyli et al. 2004) and assumed to be connected to the partial melting of lithospheric mantle with lower and middle crust due to the heat transfer from underplating mafic magma during post-collisional uplifting and extension regime combined with lithospheric delamination, lithospheric thinning and crustal contamination processes (e.g., Köksal et al. 2004, 2012; İlbeyli et al. 2004; Boztuğ et al. 2007, 2009). The latest phase of the Late-Cretaceous CACC intrusives are presumed to be alkaline rocks formed in advanced stages of the crustal extension with significant mantle component and exemplified by Bayındır–Akpınar (Kaman) alkaline rocks (e.g., Kadıoğlu et al. 2006), Buzlukdağ syenitoid (Deniz & Kadıoğlu 2016), İdiş Dağı quartz-syenitoid (Göncüoğlu et al. 1997b) and Çamsarı quartz syenitoid (Köksal et al. 2004) (Fig. 1). Some of these syenitic intrusives (e.g., Hamit: İlbeyli et al. 2004; Çamsarı: Köksal et al. 2004) coexist with the monzonitic rocks, which is attributed to the heterogeneity in the pre-collisional mantle source featured by intraplate component and pre-subduction component and/or variable involvement of continental materials (e.g., İlbeyli et al. 2004; Köksal et al. 2004). This magmatism is accompanied by Late Cretaceous volcanic rocks in some places in the complex (e.g., Karahıdır volcanic rocks; Göncüoğlu et al. 1997b) or followed by Lower Tertiary volcanism characterized by alkaline basalts, trachytes and trachy-andesites (e.g., Gökten & Floyd 1987; Çevikbaş & Öztunalı 1992; Alpaslan et al. 2004, 2006).

All these interpretations above commonly put forward the presence of granitic (granite to granodiorite), monzonitic and syenitic rocks in Central Anatolia, with different proposed sources such as subduction-modified mantle, lithospheric mantle, lower and middle crust, and several processes effective in their petrogenesis, including lithospheric delamination, slab-break-off, lithospheric thinning, crustal contamination, assimilation–fractional crystallization and mixing–mingling mechanisms.

However, these explanations do not explain the prominent crustal source, revealed mainly by isotopic data, of granitoids and gabbros in the Hacımahmutuşağı area. Köksal et al. (2013) studied the monzonitic rocks in the Satansarı area (Fig. 1) and expressed their crustal source mostly based on zircon Hf isotope data and multiple resorption zones of zircons. Köksal et al. (2013) suggested an evolution scheme for these crustal sourced-granitoids based on the Annen et al. (2006)'s petrological model, which shows similar aspects to the MASH-type models (e.g., Hildreth & Moorbath 1988; Petford & Gallagher 2001). In this model, a so called "hot zone" is formed in the deep crust due to the heat transfer from the underplated mafic magma, in the course of lithospheric thinning and delamination (i.e., fig. 9 in Köksal et al. 2013). This "hot zone" serves as a host for the water-rich magmas, which are produced by residual melts from basalt crystallization and partial melts of pre-existing crustal rocks (e.g., Paleozoic–Mesozoic–Cretaceous metamorphic and igneous rocks in the CACC) within the lower crust (Annen et al. 2006; Köksal et al. 2013). Episodic injections of these mixed melts by adiabatic ascent and crystallization in the shallow crust (e.g., Köksal et al. 2013) may give rise to the evolution of intrusives in the Hacımahmutuşağı area. Chemical and isotopic exchange probably occur during these intermittent injections and genetic character may be modified and lead to the formation of hybrid magma (e.g., Petford & Gallagher 2001). Compositional difference of these intrusive rocks (i.e., granitic and gabbroic) may point out a heterogeneity of the source of coeval rocks or subsequent gabbro intrusion with less fertile restite components (e.g., Meade et al. 2014). This kind of magma reservoir within the crust can be prolonged for a million years (e.g., Deering et al. 2016). Jackson et al. (2018) propose that reactive melt flow is a criticial mechanism in controlling magma storage, accumulation and differentiation in these long-lived mid- to lower-crustal mush reservoirs rather than fractional crystallization in magma chambers. Coeval evolution of mafic and felsic magmatic rocks is supposed to exist by differentiation of reactive melt flow in such mush reservoirs (Jackson et al. 2018). Partial melting of previously formed crustal components triggered by mafic underplating magma is possibly a phenomenon valid for the other intrusive rocks, displaying hybrid nature with a significant crustal signature, in Central Anatolia and also for the similar intrusive rocks in the world (e.g., Annen et al. 2006; Kemp et al. 2007; Barnes et al. 2012; Wang et al. 2018).

Conclusions

The findings of this study infer collisional/post-collisional character for the granitoids in the Hacımahmutuşağı area, where granite–granodiorite represents the first magmatic phase with formation of leucogranite, more crustal contamination and fractionation, following up. Both granitoids and gabbros are conceivably formed from an enriched source with a noteworthy crustal component. The coeval granitic and gabbroic rocks observed in the Hacımahmutuşağı area are likely to have been formed in shallow crust due to fractionation and episodic magmatic injections from a hot zone previously formed within the crust.

Acknowledgements: I gratefully thank Prof. Dr. Cemal Göncüoğlu for help in all stages of this study. I thank to Dr. Fatma Toksoy-Köksal for contributions in evaluation of petrographical and geochemical data, and comparison with the other gabbroic rocks in Central Anatolia. I am indebted to Prof. Dr. Mehmet Arslan for his reviews of the earlier version the manuscript. I acknowledge the Central Laboratory of Middle East Technical University for geochemical and radiogenic isotope analyses. I would like to thank Serap Tekin Kaya and

Sezen Yıldırım for geochemical analyses and Dr. Selin Süer and Sultan Atalay for their assistance in isotope analyses. Prof. Dr. Orhan Karslı, Prof. Dr. Sabah Yılmaz Şahin and Prof. Dr. Semih Gürsu are acknowledged for their constructive reviews and comments, which significantly helped to modify the manuscript.

References

Alpaslan M., Frei R., Boztuğ D., Kurt M.A. & Temel A. 2004: Geochemical and Pb–Sr–Nd isotopic constraints indicating an enriched-mantle source for Late Cretaceous to Early Tertiary volcanism, central Anatolia, Turkey. *Int. Geol. Rev.* 46, 1022–1041.

Alpaslan M., Boztuğ D., Frei R., Temel A. & Kurt M.A. 2006: Geochemical and Pb–Sr–Nd isotopic composition of the ultrapotassic volcanics from the extension-related Çamardı–Ulukışla basin, Niğde province, central Anatolia, Turkey. *J. Asian Earth Sci.* 27, 613–27.

Annen C., Bluny J.D. & Sparks R.S.J. 2006: The genesis of intermediate and silicic magmas in deep hot zones. *J. Petrol.* 47, 505–539.

Barnes C.G., Frost C.D., Nordgule Ø. & Prestvik T. 2012: Magma hybridization in the middle crust: possible consequences for deep-crustal magma mixing. *Geosphere* 8, 518–533.

Bingöl E. 1989: Geological Map of Turkey, scale 1:2.000,000. *General Directorate of Mineral Research and Exploration*, Ankara (in Turkish).

Bozkurt E. & Mittwede S. 2001: Introduction to the geology of Turkey — A Synthesis. *Int. Geol. Rev.* 43, 578–594.

Boztuğ D. 1998: Post-collisional central Anatolian alkaline plutonism, Turkey. *Turk. J. Earth Sci.* 7, 145–165.

Boztuğ D., Tichomirowa M. & Bombach K. 2007: ^{207}Pb–^{206}Pb single-zircon evaporation ages of some granitoid rocks reveal continent–oceanic island arc collision during the Cretaceous geodynamic evolution of the central Anatolian crust, Turkey. *J. Asian Earth Sci.* 31, 71–86.

Boztuğ D., Jonckheere R.C., Heizler M., Ratschbacher L., Harlavan Y. & Tichomirova M. 2009: Timing of post-obduction granitoids from intrusion through cooling to exhumation in central Anatolia, Turkey. *Tectonophysics* 473, 223–233.

Bussy F., Hernandez J. & Von Raumer J. 2000: Bimodal magmatism as a consequence of the post-collisional readjustment of the thickened Variscan continental lithosphere (Aiguilles Rouges–Mont Blanc Massifs, Western Alps). *Trans. R. Soc. Edinburgh: Earth Sci.* 91, 221–233.

Cox K.G., Bell J.D. & Pankhurst R.J. 1979: The Interpretation of Igneous Rocks. *George Allen & Unwin,* London, 1–450.

Çevikbaş A. & Öztunalı Ö. 1992: Geology of the Ulukışla–Çamardı (Niğde) Basin. *Bulletin of the Mineral Research and Exploration* 114, 155–172.

Deering C.D., Keller B., Schoene B., Bachmann O., Beane R. & Ovtcharova M. 2016: Zircon record of the plutonic-volcanic connection and protracted rhyolite melt evolution. *Geology* 44, 4, 267–270.

Deniz K. & Kadıoğlu Y.K. 2016: Assimilation and fractional crystallization of foid-bearing alkaline rocks: Buzlukdağ intrusives, Central Anatolia, Turkey. *Turk. J. Earth Sci.* 25, 4, 341–366.

Dirik K., Göncüoğlu M.C. & Kozlu H. 1999: Stratigraphy and pre-Miocene tectonic evolution of the southwestern part of the Sivas Basin, central Anatolia, Turkey. *Geol. J.* 34, 303–319.

Floyd P.A., Yalınız M.K. & Göncüoğlu M.C. 1998: Geochemistry and petrogenesis of intrusive and extrusive ophiolitic plagiogranites, Central Anatolian Crystalline Complex, Turkey. *Lithos* 42, 3, 4, 225–240.

Frost B.R., Barnes C.G., Collins W.J., Arculus R.J., Ellis D.J. & Frost C.D. 2001: A geochemical classification for granitic rocks. *J. Petrol.* 42, 2033–2048.

Gökten E. & Floyd P.A. 1987: Geochemistry and tectonic environment of the Sarkisla area volcanic rocks in central Anatolia, Turkey. *Mineral. Mag.* 51, 533–559.

Göncüoğlu M.C. 1986: Geochronological data from the southern part (Niğde area) of the Central Anatolian Massif. *Bulletin of the Mineral Research and Exploration* 105/106, 83–96.

Göncüoğlu M.C. & Türeli T.K. 1994: Alpine collision-type granitoids in the western Central Anatolian Crystalline Complex. *J. Kocaeli Univ.* 1, 39–46.

Göncüoğlu M.C., Erler A., Toprak V., Olgun E., Yalınız K., Kuşçu İ., Köksal S. & Dirik K. 1993: The geology of the Middle Section of the Central Anatolian Massif, part 3: Geological evolution of the Middle Kızılırmak Tertiary Basin. *Turkey Petroleum Corporation General Directorate*, Open file Report No. 3313, Ankara, 1–104 (in Turkish).

Göncüoğlu M.C., Dirik K. & Kozlu H. 1997a: General characteristics of pre-Alpine and Alpine Terranes in Turkey: explanatory notes to the terrane map of Turkey. *Annales Geologique de Pays Hellenique* 37, 515–536.

Göncüoğlu M.C., Köksal S. & Floyd P. A. 1997b: Post-collisional A-Type magmatism in the Central Anatolian Crystalline Complex: petrology of the İdiş Dağı intrusives (Avanos, Turkey). *Turk. J. Earth Sci.* 6, 2, 65–76.

Göncüoğlu M.C., Sayıt K. & Tekin U.K. 2010: Oceanization of the northern Neotethys: Geochemical evidence from ophiolitic melange basalts within the İzmir–Ankara suture belt, NW Turkey. *Lithos* 116, 175–187.

Göncüoğlu M.C., Tekin U.K., Sayıt K., Bedi Y. & Uzunçimen-Keçeli S. 2015: Evolution of the Neotethyan branches in the Eastern Mediterranean: Petrology and ages of oceanic basalts. In: IGCP589. The Fourth Symposium of the International Geosciences. *Programme Abstracts and Proceedings,* 17–19.

Görür N., Oktay F.Y., Seymen İ. & Şengör A.M.C. 1984: Paleotectonic evolution of Tuzgölü basin complex, central Turkey. In: Dixon J.E. & Robertson A.H.F. (Eds.): The geological evolution of the eastern Mediterranean. *Geol. Soc. London, Spec. Publ.* 17, 81–96.

Güleç N. 1994: Rb–Sr Isotope data from the Ağaçören granitoid (East of Tuz Gölü): geochronological and genetical implications. *Turk. J. Earth Sci.* 3, 39–43.

Güleç N. & Kadıoğlu Y.K. 1998: Relative involvement of mantle and crustal components in the Ağaçören Granitoid (central Anatolia -Turkey): estimates from trace element and Sr-isotope data. *Chemie der Erde* 58, 23–37.

Güleç N., Toprak V., Kadıoğlu Y.K. & Barreiro B. 1996: The anatomy of a gabbro body and its bearings on the origin of mafic enclaves in the Ağaçören granitoid (central Turkey). *Israel Journal of Earth Sciences* 45, 169–192.

Hart S.R. 1988: Heterogeneous mantle domains: signatures, genesis, and mixing chronologies. *Earth Planet. Sci. Lett.* 90, 273–296.

Harris N.B.W., Pearce J.A. & Tindle A.G. 1986: Geochemical characteristics of collision-zone magmatism. In: Coward M.P. & Alison C. (Eds.): *Geol. Soc. London, Spec. Publ.* 19, 67–81.

Hildreth W. & Moorbath S. 1988: Crustal contributions to arc magmatism in the Andes of central Chile. *Contrib. Miner. Petrol*. 98 455–489.

İlbeyli N., Pearce J.A., Thirlwall M.F. & Mitchell J.G. 2004: Petrogenesis of collision-related plutonics in central Anatolia, Turkey. *Lithos* 72, 163–182.

Irvine T.N. & Baragar W.R.A. 1971: A guide to the geochemical classification of the common volcanic rocks. *Can. J. Earth Sci.* 8, 523–548.

Jackson M.D., Blundy J. & Sparks R.S.J. 2018: Chemical differentiation, cold storage and remobilization of magma in the Earth's crust. *Nature* 564, 405–409.

Kadıoğlu Y.K. & Güleç N. 1996: Structural setting of Gabbros in the Ağaçören Granitoid: Implications from Geological and Geophysical (Resistivity) Data. *Turk. J. Earth Sci.* 5, 153–159.

Kadıoğlu Y.K. & Güleç N. 1998: The role of anorthite contents on the generation of granitoid, enclaves and gabbro in the Ağaçören Intrusive Suite: Central Anatolia, Turkey. *Mineral. Mag.* 2A, 733–734.

Kadıoğlu Y.K. & Güleç N. 2001: Gabbro Types in the Central Anatolian Crystalline Complex: Field Aspects, Petrographic Features and Geochemistry. In: Fourth International Turkish Geology Symposium, Abstract, 206.

Kadıoğlu Y.K. & Özsan A. 1997: Determination of the deep structure of gabbros in Sulakyurt granitoid by drilling. *Geological Bulletin of Turkey* 41, 177–185 (in Turkish).

Kadıoğlu Y.K., Ateş A. & Güleç N. 1998a: Structural interpretation of gabbroic rocks in Ağaçören Granitoid, Central Turkey: field observations and aeromagnetic data. *Geol. Mag.* 135, 2, 245–254.

Kadıoğlu Y.K., Kurt H. & Arslan M. 1998b: Determination of Ophiolitic and nonophiolitic gabbroic rocks in Central Anatolia using the Cr/Si ratio in clinopyroxene. *Mineral. Mag.* 2A, 735–736.

Kadıoğlu Y.K., Dilek Y., Güleç N. & Foland K.A. 2003: Tectonomagmatic evolution of bimodal plutons in the Central Anatolian Crystalline Complex, Turkey. *J. Geol.* 111, 671–690.

Kadıoğlu Y.K., Dilek Y. & Foland K.A. 2006: Slab break-off and syncollisional origin of the Late Cretaceous magmatism in the Central Anatolian Crystalline Complex, Turkey. In: Dilek Y. & Pavlides S. (Eds.): Postcollisional tectonics and magmatism in the Mediterranean region and Asia. *Geol. Soc. Am. Spec. Pap.* 409, 381–415.

Kelemen P.B., Shimizu N. & Dunn T. 1993: Relative depletion of niobium in some arc magmas and the continental crust: partitioning of K, Nb, La and Ce during melt/rock reaction in the upper mantle. *Earth Planet. Sci. Lett.* 120, 3–4, 111–134.

Kemp A.I.S., Hawkesworth C.J., Foster G.L., Paterson B.A., Woodhead J.D., Hergt J.M., Gray C.M. & Whitehouse M.J. 2007: Magmatic and crustal differentiation history of granitic rocks from Hf-O isotopes in zircon. *Science* 315, 980–983.

Koçak K., Işık F., Arslan M. & Zedef V. 2005: Petrological and source region characteristics of ophiolitic hornblende gabbros from the Aksaray and Kayseri regions, central Anatolian crystalline complex, Turkey. *J. Asian Earth Sci.* 25, 883–891.

Köksal S. 1992: Geology and petrography of Hacımahmutuşağı region (Ortaköy-Aksaray). *B.Sc. Thesis, Middle East Technical University*, Ankara, 1–54.

Köksal S. & Göncüoğlu M.C. 2008: Sr and Nd isotopic characteristics of some S-, I- and A-type granitoids from Central Anatolia. *Turk. J. Earth Sci.* 17, 111–127.

Köksal S., Göncüoğlu M.C. & Toksoy-Köksal F. 2001: The geological and petrographical characteristics of the magmatic rocks and their contact zones in the Hacımahmutusağı (Ortaköy-Aksaray) area, Central Anatolian Crystalline Complex, Turkey. *Fourth International Turkish Geology Symposium, Work in Progress on the Geology of Turkey and Its Surroundings*, *2001, Çukurova University*, Adana, 216.

Köksal S., Romer R.L., Göncüoğlu M.C. & Toksoy-Köksal F. 2004: Timing of the transition from the post-collisional to A-type magmatism: titanite U/Pb ages from the alpine Central Anatolian Granitoids, Turkey. *Int. J. Earth Sci.* 93, 974–989.

Köksal S., Möller A., Göncüoğlu M.C., Frei D. & Gerdes A. 2012: Crustal homogenization revealed by U-Pb zircon ages and Hf isotope evidence from the Late Cretaceous granitoids of the Agaçören intrusive suite (Central Anatolia/Turkey). *Contrib. Mineral. Petrol.* 163, 725–743.

Köksal S., Toksoy-Köksal F., Göncüoğlu M.C., Möller A., Gerdes A. & Frei D. 2013: Crustal source of the Late Cretaceous Satansarı monzonite (Central Anatolia/Turkey) and its significance for the Alpine geodynamic evolution. *J. Geodyn.* 65, 82–93.

Köksal S., Toksoy-Köksal F. & Göncüoğlu M.C. 2017: Petrogenesis and geodynamics of plagiogranites from Central Turkey (Ekecikdağ/Aksaray): new geochemical and isotopic data for generation in an arc basin system within the northern branch of Neotethys. *Int. J. Earth Sci. (Geol. Rundsch.)* 106, 1181–1203..

McDonough W.F. & Sun S-S. 1995: The composition of the earth. *Chem. Geol.* 120, 223–253.

Meade F.C., Troll V.R., Ellam R.M., Freda C., Font L., Donaldson C.H. & Klonowska I. 2014: Bimodal magmatism produced by progressively inhibited crustal assimilation. *Nature Communications* 5, art. no. 4199.

Miller C., Thöni M., Goessler W. & Tessadri R. 2011: Origin and age of the Eisenkappel gabbro to granite suite (Carinthia, SE Austrian Alps). *Lithos* 125, 434–448.

Moix P., Beccaletto L., Kozur H.W., Hochard C., Rosselet F. & Stampfli G.M. 2008: A new classification of the Turkish terranes and sutures and its implication for the Paleotectonic history of the region. *Tectonophysics* 451, 7–39.

Okay A.İ. & Tüysüz O. 1999: Tethyan sutures of northern Turkey. In: Durand, B., Jolivet, L., Horwarth, E., Seranne, M. (Eds.): The Mediterranean Basins: Tertiary Extension within the Alpine Orogen. *Geol. Soc. London, Spec. Publ.* 156, 475–515.

Pearce J.A. 1996: Sources and settings of granitic rocks. *Episodes* 19, 120–125.

Pearce J.A. 2008: Geochemical fingerprinting of oceanic basalts with applications to ophiolite classification and the search for Archean oceanic crust. *Lithos* 100, 14–48.

Pearce J.A., Harris N.B.W. & Tindle A.G.W. 1984: Trace element discrimination diagrams for the tectonic interpretation of granitic rocks. *J. Petrol.* 25, 956–983.

Petford N. & Gallagher K. 2001: Partial melting of mafic (amphibolitic) lower crust by periodic influx of basaltic magma. *Earth Planet. Sci. Lett.* 193, 3–4, 483–499.

Pitcher W.S. 1979: The nature, ascent and emplacement of granite magmas. *J. Geol. Soc. London* 136, 627–662.

Robertson A.H.F., Parlak O. & Ustaömer T. 2009: Melange genesis and ophiolite emplacement related to subduction of the northern margin of the Tauride–Anatolide continent, central and western Turkey. In: Van Hinsbergen D.J.J., Edwards M.A., Govers R. (Eds.): Collision and collapse at the Africa–Arabia–Eurasia Subduction Zone. *Geol. Soc. London, Spec. Publ.* 311, 9–66.

Seymen İ. 1981: The stratigraphy and metamorphism of the Kırşehir Massif near Kaman (Kırşehir). *Bulletin of the Geological Society of Turkey* 24, 7–14 (in Turkish).

Sun S-S. & McDonough W.F. 1989: Chemical and isotopic systematics of oceanic basalts; implications for mantle composition and processes. In: Saunders, A.D., Norry, M.J. (Eds.): Magmatism in the ocean basins. *Geol. Soc. London, Spec. Publ.* 42, 313–345.

Toksoy-Köksal F. 2016: Petrogenesis of the Ekecikdağ Magmatic Associaton (Central Anatolia): Mineral Chemistry Perspective. *Bulletion of the Earth Sciences Application and Research Centre of Hacettepe University* 37, 2, 139–178 (in Turkish).

Toksoy-Köksal F. 2019: On the geodynamics of the Alpine collisional granitoids from Central Anatolia: petrology, age and isotopic characteristics of the granitoids of the Ekecikdağ Igneous Association (Aksaray/Turkey). *Geodin. Acta* 31, 1–26.

Toksoy-Köksal F., Oberhaensli R. & Göncüoğlu M.C. 2009: Hydrous aluminosilicate metasomatism in an intra-oceanic subduction zone: Implications from the Kurançalı (Turkey) ultramafic–mafic cumulates within the Alpine Neotethys Ocean. *Mineral. Petrol.* 95, 273–290.

Toksoy-Köksal F., Köksal S. & Göncüoğlu M.C. 2010: Is a single model adequate to explain origin of the gabbros from Central Anatolia, Turkey? In: Symposium of Geological Society of America, Tectonic Crossroads: Evolving Orogens of Eurasia–Africa–Arabia, 2010. Ankara, 83.

van Hinsbergen D.J.J., Maffione M., Plunder A., Kaymakçı N., Ganerød M., Hendriks B.W.H., Corfu F., Gürer D., de Gelder G.I.N.O., Peters K., McPhee P.J., Brouwer F.M., Advokaat E.L. & Vissers R.L.M. 2016: Tectonic evolution and paleogeography of the Kırşehir Block and the Central Anatolian Ophiolites, Turkey. *Tectonics* 35, 4, 983–1014.

Wang L.J., Guo J.H., Yin C., Peng P., Zhang J., Spencer C.J. & Qian J.H. 2018: High-temperature S-type granitoids (charnockites) in the Jining complex, North China Craton: Restite entrainment and hybridization with mafic magma. *Lithos* 320–321, 435–453.

Whitney D.L., Teyssier C., Fayon A.K., Hamilton M.A. & Heizler M. 2003: Tectonic controls on metamorphism, partial melting, and intrusion: timing and duration of regional metamorphism and magmatism in the Niğde Massif, Turkey. *Tectonophysics* 376, 37–60.

Yalınız M.K., Aydın N.S., Göncüoğlu M.C. & Parlak O. 1999: Terlemez quartz monzonite of Central Anatolia (Aksaray-Sarıkaraman): age, petrogenesis and geotectonic implications for ophiolite emplacement. *Geol. J.* 34, 233–242.

Yalınız M.K., Göncüoğlu M.C. & Özkan-Altıner S. 2000: Formation and emplacement ages of the SSZ-type Neotethyan Ophiolites in Central Anatolia, Turkey: paleotectonic implications. *Geol. J.* 35, 53–68.

Zindler A. & Hart S.R. 1986: Chemical Geodynamics. *Annual Review of Earth and Planetary Sciences* 14, 493–571.